

Molecular characterization of the receptor binding structure-activity relationships of influenza B virus hemagglutinin

V. CARBONE¹, H. KIM², J. X. HUANG³, M. A. BAKER⁴, C. ONG⁵, M. A. COOPER³, J. LI⁶, S. ROCKMAN⁵, T. VELKOV^{6*}

¹AgResearch, Grasslands Research Centre, Palmerston North 4442, New Zealand; ²Burnet Institute, Prahran, Victoria, Australia, 3004;

³Institute for Molecular Bioscience The University of Queensland 306 Carmody Road St Lucia QLD 4072; ⁴Priority Research Centre in Reproductive Science, School of Environmental and Life Sciences, University of Newcastle, Callaghan, NSW, 2308, Australia;

⁵CSL Limited Poplar Road, Parkville, Victoria 3052, Australia; ⁶Drug Delivery, Disposition and Dynamics, Monash Institute of Pharmaceutical Sciences, Monash University, 381 Royal Parade, Parkville 3052, Victoria, Australia

Received December 12, 2012; accepted July 8, 2013

Summary. – Selectivity of α 2,6-linked human-like receptors by B hemagglutinin (HA) is yet to be fully understood. This study integrates binding data with structure-recognition models to examine the impact of regional-specific sequence variations within the receptor-binding pocket on selectivity and structure activity relationships (SAR). The receptor-binding selectivity of influenza B HAs corresponding to either B/Victoria/2/1987 or the B/Yamagata/16/88 lineages was examined using surface plasmon resonance, solid-phase ELISA and gel-capture assays. Our SAR data showed that the presence of asialyl sugar units is the main determinant of receptor preference of α 2,6 versus α 2,3 receptor binding. Changes to the type of sialyl-glycan linkage present on receptors exhibit only a minor effect upon binding affinity. Homology-based structural models revealed that structural properties within the HA pocket, such as a glyco-conjugate at Asn194 on the 190-helix, sterically interfere with binding to avian receptor analogs by blocking the exit path of the asialyl sugars. Similarly, naturally occurring substitutions in the C-terminal region of the 190-helix and near the N-terminal end of the 140-loop narrows the horizontal borders of the binding pocket, which restricts access of the avian receptor analog LSTa. This study helps bridge the gap between ligand structure and receptor recognition for influenza B HA; and provides a consensus SAR model for the binding of human and avian receptor analogs to influenza B HA.

Keywords: influenza B; receptor binding; structure-activity relationships

Introduction

The influenza surface glycoprotein haemagglutinin (HA) binds to sialylglycoproteins and sialylglycolipids on the

surface of host cells (Gambaryan *et al.*, 1997; Stevens *et al.*, 2006a). These sialyl-glycans, usually linked to galactose (Gal) in either α 2,6 or α 2,3 configurations, are the receptors for the viral HA, the binding to which promotes viral attachment, membrane fusion and internalization of the virus (Skehel and Wiley, 2000; Suzuki, 2005). For influenza A viruses, the host glycan distribution and binding specificity of the viral HA to these sialyl-glycans is a major determinant of the host range for the virus, with avian viruses displaying a preference for α 2-3 linked sialyl-glycans and human viruses preferentially binding α 2-6 linked sialyl-glycans (Gambaryan *et al.*, 1997; Suzuki, 2005; Stevens *et al.*, 2008).

Whilst the molecular determinants of receptor specificity of the different subtypes of influenza A virus HAs have been well characterized, there have been few studies characterising the receptor-binding relationships of influ-

*Corresponding authors. E-mail: Tony.Velkov@monash.edu; phone: +61-3-9903-9539.

Abbreviations: BPL = β -propiolactone; DSLNT = Disialyllacto-N-tetraose; HA = hemagglutinin; Le^a = Lewis sugar A; LSTa = sialyllactose-N-tetraose a; LSTb = N-Acetylneuramin-lacto-N-tetraose b; LSTc = sialyllactose-N-tetraose c; Neu5A = N-Acetylneuraminic acid; MSLNH = Monosialyllacto-N-hexaose; 3'-SL = 3'-sialyl(N-acetyllactose); 6'-SL = 6'-sialyl(N-acetyllactose); SLe^a = 3'-Sialyl-Lewis-a tetrasaccharide; SLe^x = 3'-Sialyl-Lewis-X tetrasaccharide; 3'-SLN = 3'-sialyl(N-acetyllactoseamine); 6'-SLN = 6'-sialyl(N-acetyllactoseamine); SLNFPI = Sialyllacto-N-fucopentaose I

enza B virus HAs (Matrosovich *et al.*, 1993; Gambaryan *et al.*, 1999; Lugovtsev *et al.*, 2009). In contrast to the broad host range of influenza A strains, B viruses circulate exclusively in humans. One major gap in our understanding is if this host-restriction arises from preferential binding to α 2,6 sialyl-glycans in the human respiratory tract and the sialyl-glycan linkage selectivity of influenza B HA (Suzuki, 2005). Previously, the lack of crystal structures of influenza B HA-receptor complexes and the low sequence homology with influenza A HA sub-types, for which there is extensive crystallographic data for HA-receptor complexes (Skehel and Wiley, 2000; Gamblin *et al.*, 2004; Stevens *et al.*, 2006b; Xu *et al.*, 2010), has hampered our understanding of how the influenza B HA influences host receptor selectivity. Recently, the first crystal structure of an influenza B virus HA, B/HongKong/8/1973, in complex with α 2,3-linked avian-like (LSTa) and α 2,6-linked human-like (LSTc) human receptor analogs has been reported (Wang *et al.*, 2007, 2008). Surprisingly, these structures, which remain the only crystallographic complexes for influenza B virus HAs, revealed that the receptor-binding pocket is capable of making optimal contacts equally well with both receptor analogs (Wang *et al.*, 2007).

Currently, there are two major lineages of influenza B viruses in circulation, namely B/Victoria/2/1987 and B/Yamagata/16/1988 (Kanegae *et al.*, 1990; Nerome *et al.*, 1998). Importantly, viruses from the two influenza B lineages exhibit naturally occurring amino acid substitutions that cluster within the binding pocket of HA that may alter receptor-binding affinity, and hence selectivity of the respective influenza B lineages. This study examines the impact of regional-specific variations within the receptor-binding pocket of influenza B virus HA and the impact of these variations on receptor-binding selectivity. The receptor-binding selectivity of influenza B HAs corresponding to either B/Victoria/2/1987 (B/Brisbane/60/2008 and B/Malaysia/2506/2004) or, B/Yamagata/16/88 (B/Florida/4/2006) lineages was examined using a surface plasmon resonance (SPR), solid-phase ELISA and gel-capture assays. Homology-based structural models were constructed of the HAs in complex with LSTc (human) and LSTa (avian) pentasaccharide receptor analogs to ascertain the correlation between amino acid differences within the binding pocket of the three influenza B viruses with binding to different receptor analogs.

Materials and Methods

Materials. Receptor analogs Neu5A, 3'-SL, 6'-SL, 6'-SLN, DSLNT, LSTa, LSTb, LSTc, 3'-SL-ADP-HSA, 6'-SL-ADP-HSA, SLe^a, SLe^x, Le^a, SLNFPI, MSLNH, and LST-fractogels (Table 1 and Fig. 7) were either from IsoSep AB (Tullinge, Sweden) or

Sigma-Aldrich (Melbourne, Australia). Biotinylated 3'-SL and 6'-SLN were obtained from Glycotech (Maryland, USA). C1 Biacore chips were obtained from GE Heath Care (Melbourne, Australia). Nunc immobilizer 96 well-plates were obtained from Thermo Fisher Scientific (Melbourne, Australia). All materials and chemicals were of the highest commercial quality available.

Viruses. Viruses were propagated either in the allantoic cavities of 10-day-old embryonated chicken eggs (2 passages) or Madin-Darby canine kidney (MDCK) cells (5 passages). MDCK cells were maintained in minimal essential medium supplemented with 10% fetal calf serum at 37°C and 5% CO₂. Viruses were quantified by the hemagglutination assay (Szretter *et al.*, 2006). Hemagglutination titers were determined by standard procedure using chicken red blood cells in PBS (Szretter *et al.*, 2006).

Surface plasmon resonance. SPR experiments were performed in PBS running buffer using a Biacore 3000 instrument (GE Health Care, Melbourne, Australia). Influenza virus particles were immobilized on a C1 sensor chip. After the activation of surface carboxyl groups using a 1:1 mixture of 1-ethyl-3-(3-dimethylaminopropyl)carbodiimide hydrochloride (1 mol/l) and N-hydroxysuccinimide (0.25 mol/l), virus particles were diluted in 0.1 mol/l sodium acetate pH 4.0, and injected across the chip surface at a flow rate of 5 μ l/min. The immobilization level was usually around 1500~2500 response units (RUs). Then a concentration series of 3'- or 6'-SL-ADP-human serum albumin conjugate (3'- or 6'-SL-ADP-HSA) were injected across the virus immobilized surfaces and a blank reference surface at a flow rate of 20 μ l/min. The mol of oligosaccharide per mol of protein was determined from the dry weight of oligosaccharide following conjugation. 3'-SL-ADP-HSA had 22 mol oligosaccharide/mol protein; 6'-SL-ADP-HSA had 15 mol oligosaccharide/mol protein. The molecular weights of the conjugates were also evaluated by MALDI-TOF mass spectrometry (Ultraflex Extreme, Bruker). Analytes (bound receptors) were removed following each binding reaction using duplicate 20 μ l pulses of 50 mmol/l NaOH at 30 μ l/min. HSA was used as a control analyze, which didn't show any binding to the immobilized viruses. Each concentration was repeated at least 3 times. Data analysis and fitting was performed using GraphPad Prism V5.0 (www.GraphPad.com).

Gel capture assay. This procedure was performed essentially as previously described with minor modifications to the original protocol (Velkov *et al.*, 2011). Viruses in PBS were standardized to 150 μ g/mL HA protein and 100 μ l aliquots were incubated with 10–100 μ l of either LSTa or LSTc fracto-gel slurry (approximately 2.0 μ mol/g substitution, determined by weight of oligosaccharide after substitution) at 4°C for 30 min. For the competition experiments, increasing concentrations of free receptor analogs were incubated with the virus at 4°C for 30 min, before the mixture was combined with 100 μ l of LST-gel slurry. The sialidase inhibitor oseltamivir (10 μ mol/l) was included in all incubations. The gel slurry was sedimented by centrifuga-

Table 1. (continued)

Sialylated oligosaccharide	K_i ($\mu\text{mol/l}$)								
	ELISA			Gel-capture			SPR		
	B/Brisbane	B/Malaysia	B/Florida	B/Brisbane	B/Malaysia	B/Florida	B/Brisbane	B/Malaysia	B/Florida
Sialyllacto-N-fucopentaose I (SLNFPI)									
Neu5Aca2	² NB	² NB	² NB	² NB	² NB	² NB	³ ND	³ ND	³ ND
6									
Gal β 1-3GlcNAc β 1-3Gal β 1-4Glc									
2									
Fuca1									
Monosialyllacto-N-hexaose (MSLNH)									
Neu5Aca2	² NB	² NB	² NB	² NB	² NB	² NB	³ ND	³ ND	³ ND
6									
Gal β 1-4GlcNAc β 1									
\									
6									
Gal β 1-4Glc									
3									
/									
Gal β 1-3GlcNAc β 1									

¹ K_d values determined by measuring sialyl-oligosaccharide binding directly (non-competition). ²NB No binding detected. ³ND Not determined. ⁴ K_i values determined using MDCK-passaged influenza B viruses.

tion at 6,000 x g for 1 min and washed four times with 300 μl PBS. Captured virus was released with 100 μl reducing SDS-PAGE sample buffer, vortexed and heated for 1 min at 95°C. Approximately 10 μl was sampled and resolved by SDS-PAGE on 4–20% polyacrylamide Tris-Glycine gels. Gels were silver stained to visualize proteins. Gels were dried between cellulose sheets and scanned at 1200 dpi. Protein bands were quantified densitometrically using LabImage 1D gel analysis software V3.4 (Kapelán GmbH, www.kapelan-bioimaging.com). Binding inhibition constants (K_i) for analog binding were determined by non-linear regression fitting of the densitometric data to a one-site binding model as previously described in detail (Velkov *et al.*, 2011).

ELISA solid-phase assay. This procedure was performed using the biotinylated 3'-SL and 6'-SL, essentially as previously described with minor modifications to the original protocol (Chandrasekaran *et al.*, 2008; Srinivasan *et al.*, 2008). In brief, Nunc immobilizer 96 well-plates were coated with influenza virus (0.1 mg/ml HA) and blocked with 1% BSA. Various dilutions of biotinylated sialyl-glycans at the desired concentrations in PBS were added into the wells (50 μl /well) and the plates were incubated at 4°C for 1 hr. For the competition experiments, increasing concentrations of free receptor analogs were added to the incubation mixture containing a saturating concentration (5 $\mu\text{mol/l}$) of biotinylated 3'-SL or 6'-SLN. To inhibit viral sialidase activity, oseltamivir (10 $\mu\text{mol/l}$) was included in all

wells. The wells were washed four times with PBS and bound biotinylated sialyl-glycans were quantified with 25 μl /well of HRP-streptavidin (1:2,000). Plates were incubated at 4°C for 1 hr. After washing with PBS, the peroxidase activity was assayed with O-phenylenediamine solution and the reaction was stopped with 50 μl of 1 mol/l HCl. Absorbance was determined at 490 nm. The apparent affinity constant (K_D) for virus binding to 3'-SL and 6'-SLN was determined from the non-linear regression fit of the plot of biotinylated sialyl-glycan concentration versus the A_{490} to a standard binding hyperbola generated using GraphPad Prism V5.0 software.

Viral HA gene sequencing and analysis. Total RNA was isolated from the allantoic fluid of infected embryonated chicken eggs using the RNeasy mini-kit (Qiagen, Melbourne, Australia) as per the manufacturer's instructions. RT-PCR was performed with genome-specific primers and the resultant cDNA sequenced using a DNA ABI Prism 3130 sequencer (Applied Biosystems) and BigDye Terminator v3.1 kit. DNA sequences were completed and edited using DNASTAR sequence analysis software (DNASTAR, Inc.). Multiple sequence alignments and percentage sequence identity (PID) calculations were performed using the CLUSTAL W program (Thompson *et al.*, 1994; May, 2004).

Homology modeling of the influenza B HA structures. Structural models of the influenza B HA molecules were constructed using the experimental crystal structures of B/Hong Kong/8/1973 HA in complex with the human receptor analog LSTc (RCSB Protein Data

Bank www.rcsb.org/pdb; PDB ID: 2RFU) and avian receptor analog LSTa (PDB ID: 2RFT) as the modeling templates (Wang *et al.*, 2007). The models were constructed using macromodel as implemented in the Maestro Schrödinger Suite 2008 (Schrödinger, NY, USA). The quality of the models was evaluated with the WHAT-CHECK program (Hooft *et al.*, 1996). All structural representations were generated with the molecular viewer PyMol v0.99 (<http://www.pymol.org>).

In silico docking. Molecular docking experiments were carried out using the program GOLD (Genetic Optimization for Ligand Docking), Version 5.0 (Verdonk 2003). For each GOLD run the binding site was composed of all residues that fell within 5 Å of the center of the influenza B HA RBS highlighting interactions with the conserved residues Phe95, Trp158, His191, Leu201, and Pro238. Side-chain residues were rigid and no water molecules were defined as part of the active site. The diverse solutions option of GOLD was turned on (Cluster size 2, RMSD 2) with automatic GA settings of 20 and with a 100% search efficiency. A Piecewise Linear Potential (PLP) scoring option was the preferred function using default parameters. Per atom scoring was enabled and tracked.

Results and Discussion

Human versus avian analog binding selectivity of the influenza B virus HA variants

The human versus avian receptor specificity of the three influenza B virus HA variants were determined using solid-phase ELISA, LST gel-capture and SPR assays to measure viral HA binding to sialyl-oligosaccharide analogs representative of avian (3'-SL, LSTa) and human (6'-SL, 6'-SLN, LSTc) receptors (Table 1 and Fig. 7). The SPR assay is limited to measuring HA-probe interactions directly (which yield dissociation constants, K_D values), whereas the gel-capture and ELISA methods were employed for measuring direct binding affinity, as well as in competition studies using free receptor analogs (which yield inhibitory dissociation constants, K_i values).

The SPR assay measured binding of the viral HA to the trisaccharide 3'-SL or 6'-SL analogs that are covalently attached to human serum albumin (HSA), which is amine coupled to the chip surface (cf. Fig 1c, d insets). Sensorgrams were normalized using a reference sensorgram consisting of an inactivated blank carboxylated surface. Resultant SPR sensorgrams indicated that all three viruses bound 3'-SL and 6'-SL analogs equally well with a similar dose-dependent response for each virus (Fig. 1a,b and Fig. 8). Binding data points were obtained just before the end of each injection for K_D calculations using a MW of 70 kDa for the sialyloligosaccharide-HSA conjugates. The K_D results indicate that the rank order of affinity for both 3'-SL and 6'-SL decreases in

the order B/Malaysia/2506/2004 \geq B/Florida/4/2006 \gg B/Brisbane/60/2008 (Fig. 1c,d and Table 1). The HA of B/Malaysia/2506/2004 and B/Florida/4/2006 displayed a comparable binding affinity range ($K_D = 0.2 \rightarrow 0.4 \mu\text{mol/l}$) for both receptor analogs, whereas B/Brisbane/60/2008 showed an approximately 4-fold lower affinity for each receptor ($K_D = 0.8 \rightarrow 1.7 \mu\text{mol/l}$) (Table 1).

The K_D affinity constants calculated from the ELISA direct binding measurements indicated that all three viruses exhibited marginally greater preference for 6'-SLN (human analog) over 3'-SL (avian analog) (Table 1). Similarly, the results from the LST gel-capture assay experiments that measured virus binding directly to the gel-immobilized LST analogs showed all three strains display a stronger preference for LSTc (human analog) compared to LSTa (avian analog) (Table 1).

We then performed competition experiments using gel-capture and ELISA assay platforms, where increasing concentrations of free receptor analogs are used to displace the biotinylated probe (ELISA) or gel-bound virus (gel-capture), from which inhibitory dissociation constants are derived (Figs. 2 and 3; Table 1). The ELISA and gel-capture competition data revealed that the binding affinity for the human receptor analogs 6'-SL, 6'-SLN and LSTc decreased in the order B/Florida/4/2006 $>$ B/Malaysia/2506/2004 $>$ B/Brisbane/60/2008. On the other hand, the binding affinity for the avian receptor analogs 3'-SL, 3'-SLN and LSTa decreased in the rank order B/Malaysia/2506/2004 $>$ B/Florida/4/2006 $>$ B/Brisbane/60/2008. In both the ELISA and gel-capture competition assays, B/Florida/4/2006 and B/Brisbane/60/2008 exhibited a greater binding affinity for LSTc (human receptor analog) than the LSTa (avian receptor analog), whereas B/Malaysia/2506/2004 exhibited a comparable affinity for both analogs (Table 1). Moreover, B/Malaysia/2506/2004 and B/Florida/4/2006 displayed an overall higher affinity for the analogs compared to B/Brisbane/60/2008. Notably, the binding affinity of the LST analogs was much higher when the analogs were free in solution (competition assay) compared to experiments, where the analogs were coupled to the gel by their asialyl terminal sugar unit (gel-capture direct binding assay). This was particularly the case with LSTa, where the difference in affinity between the direct and competition experiments was >10 -fold and suggests that the coupling of terminal sugars to the receptor analogs negatively impacts HA binding.

It is well established that propagation of influenza B viruses for more than 3 passages results in egg-adaptive mutations in the HA, such as the loss of the N-glycosylation site at position 194–196 (Robertson *et al.*, 1993; Saito *et al.*, 2004). Egg-adapted variants are not representative of the virus circulating in the human population and often display altered receptor-binding properties (Gambaryan

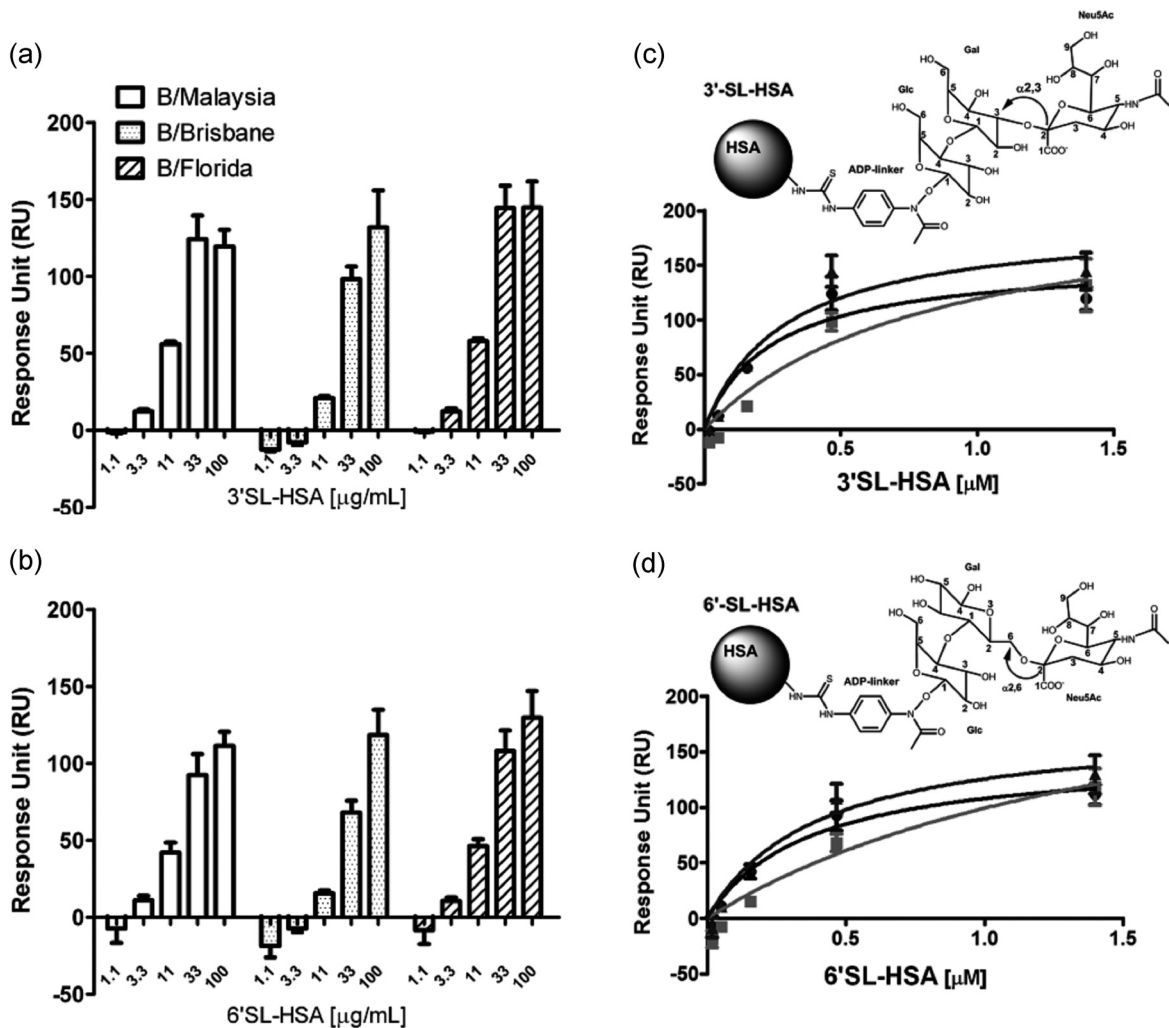


Fig. 1

SPR assay of the binding of 3'-SL-HSA and 6'-SL-HSA to immobilized influenza B viruses

(a) Binding response of 3'-SL-HSA. (b) Binding response of 6'-SL-HSA. (c), (d) Determination of binding affinity constants (K_D) for the binding of 3'-SL-HSA and 6'-SL-HSA to immobilized influenza B viruses by non-linear regression fitting of the SPR data to a one-site binding model. (●) B/Malaysia/2506/04/2004; (■) B/Brisbane/60/2008; (▲) B/Florida/4/2006.

et al., 1999; Saito *et al.*, 2004). However, it has also been shown that transient passaging of influenza B viruses (1–2 passages, as per our study) in eggs often does not result in egg-adaptive changes, such as the loss of the N-glycosylation site at position 194–196 (Rota *et al.*, 1992; Gatherer, 2010; Robertson *et al.*, 1993; Saito *et al.*, 2004). In order to ensure the HAs of the transiently egg-passaged viruses are identical to the clinical isolates, their HAs were sequenced and analyzed to ensure they match the parental isolates and have not undergone any egg-adaptation mutations. Moreover, as a control, we have included the receptor selectivity results for MDCK-propagated viruses

(5 passages) (Table 1). The resultant K_i values did not reveal any discernable differences between the MDCK- and the egg-propagated viruses, not surprisingly as their HA gene sequences are both identical with the original clinical isolates.

Structure-activity relationships (SAR)

In order to explore the SAR of the receptor-influenza B HA binding interaction, we examined the binding characteristics of an extended set of sialyl- and asialyl-oligosaccharide analogs using the ELISA and gel-capture assays

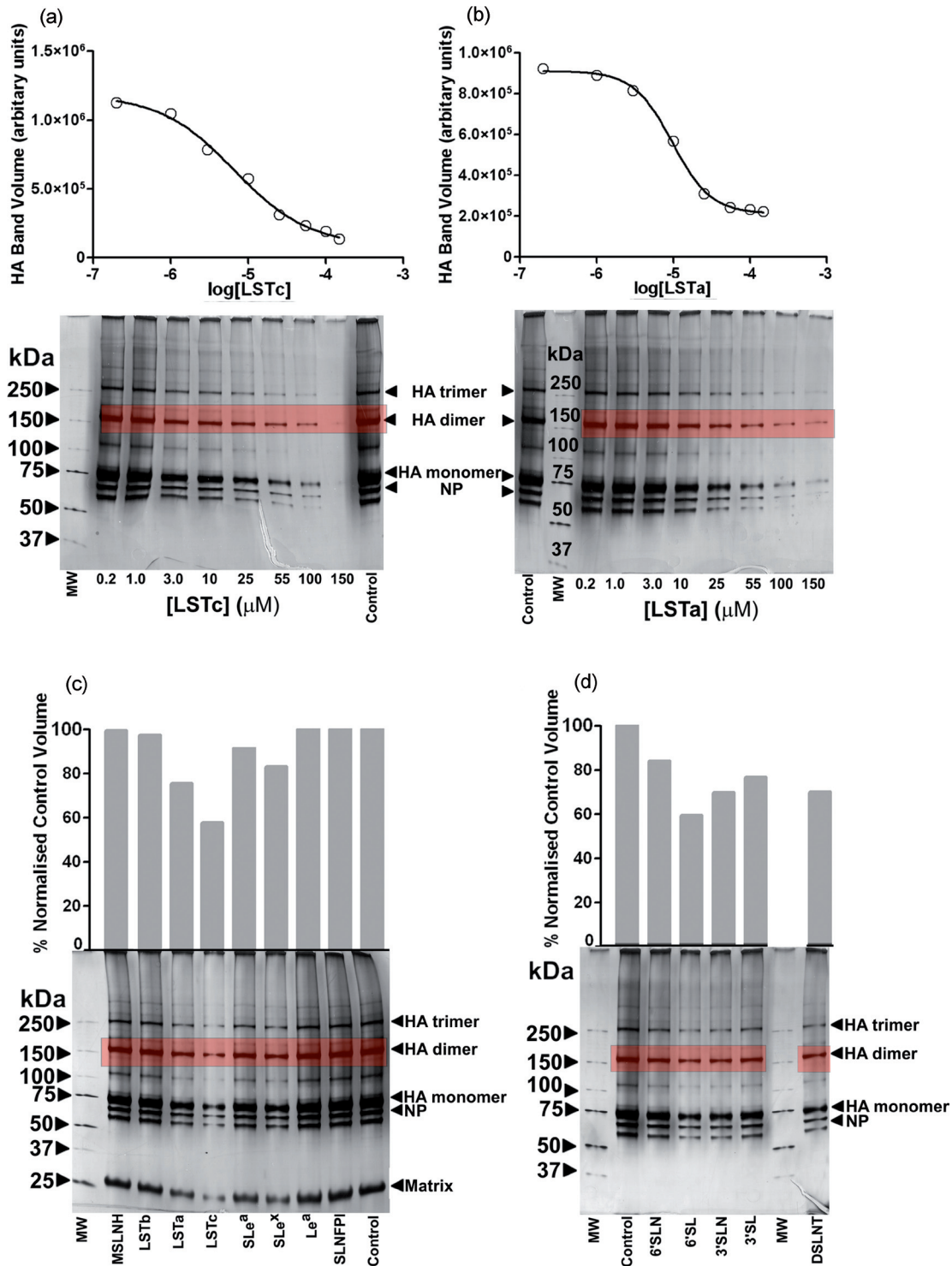


Fig. 2

Receptor selectivity of influenza B virus HA measured by a whole virus gel-capture assay

The SDS-PAGE and densitometry results for B/Florida/4/2006 are shown as example data. (a) and (b) Displacement of whole virus captured onto LSTa-gel by incubation with increasing concentrations of free LSTa or LSTc. Top panels. Determination of binding-inhibition constants (K_i) by non-linear regression fitting of the densitometric data to a one-site binding model. (c) and (d) Displacement of whole virus captured onto LSTa-gel by incubation with 20 μmol/l of each receptor analog. Top panels. The bar graphs show the densitometric quantification of HA band intensity represented as the relative percentage normalized to the control LSTa-gel capture reaction in the absence of a competing ligand.

(Figs. 2 and 3; Table 1). All three viruses displayed a binding affinity for the $\alpha 2,3/\alpha 2,6$ di-sialylated analog DSLNT that was intermediate to their respective affinities for LSTa

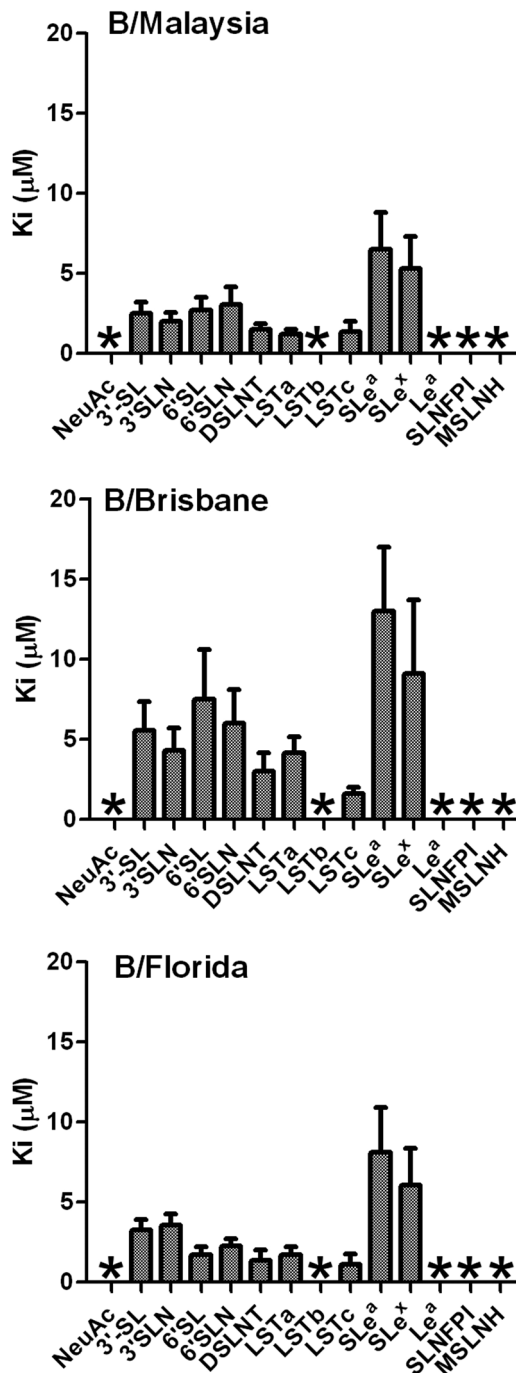


Fig. 3

Sialyl-glycan affinity profile of influenza B virus HAs measured by a whole virus gel-capture competition assay

The asterisk indicates no binding detected.

and LSTc. The binding affinity for the $\alpha 1-3$ (SLe^x) and $\alpha 1-4$ (SLe^a) fructose substituted 3'-Sialyl-Lewis tetrasaccharides was lower compared to the 3'-SL, 3'-SLN, 6'-SL and 6'-SLN trisaccharide and LST analogs (Figs. 2c,d and 3). No binding was detected with either Neu5Ac or with Neu5Ac connected to an internal GlcNAc-3 with either sugar chain (LSTb and SLFPI) or asialyl (Le^a) or branched sialyl (MSLNH) analogs (Figs. 2c and 3).

Combining the data from the three assays, we constructed a consensus SAR model for the binding of human and avian receptor analogs to influenza B HAs (Fig. 4a). We propose that: **i)** In contrast to influenza A HA-receptor interactions, where the configuration of NeuNAc-1-Gal-2 glycosidic linkage is the primary determinant for receptor-binding preference, the influenza B virus HA does not overtly discriminate between NeuNAc-1-Gal-2 glycosidic linkages in human and avian receptor analogs. **ii)** The distal asialyl Gal-4-Glc-5 sugars in the $\alpha 2,3$ avian receptor analog LSTa, which is in an extended conformation in the crystal structure with B/Hong Kong/8/1973 (cf. Fig. 5a), makes extensive contacts with the binding pocket. In contrast, the terminal sugars in the bound $\alpha 2,6$ human receptor analog LSTc, which is in a U-shaped configuration in the crystal structure with B/Hong Kong/8/1973 (cf. Fig. 5a), do not make any contacts with the binding pocket. **iii)** Interactions with the distal asialyl sugars are responsible for modulating binding avidity of avian receptor analogs. Accordingly, the use of asialyl units as coupling points to solid-phase supports or carrier molecules negatively impacts binding to avian receptor analogs, as these distal asialyl sugars are involved in binding avidity to HA. Our analysis indicates that recognition of distal asialyl sugar structure is a key mechanism, by which influenza B HA differentiates between human and avian receptor analogs. Most assays utilise sialyl-oligosaccharide receptor analogs attached to a solid-phase support or carrier molecule by the terminal sugar unit. However, these terminal sugars are involved in contacting the HA for binding and the use of either a polyvalent ligand arrangement or attachment on to a solid-phase support is likely to crowd these sugars and hinder the recognition. Accessibility to the terminal sugars appears to be more important for the binding mode of avian receptor analogs (e.g LSTa) than for the human receptor analogs (e.g LSTc). **iv)** The length of the oligosaccharide is critical for influenza B HA recognition, a disaccharide consisting of NeuNAc linked to the penultimate Gal is the minimal unit required for influenza B HA binding. The influenza B HAs did not overtly discriminate between trisaccharide human and avian receptor analogs, whereas a clear $\alpha 2,6$ over $\alpha 2,3$ receptor preference was evident with the pentasacchride analogs. Thus, an accessible asialyl terminus on the receptor analog containing an oligosaccharide of at least five sugar units in length is

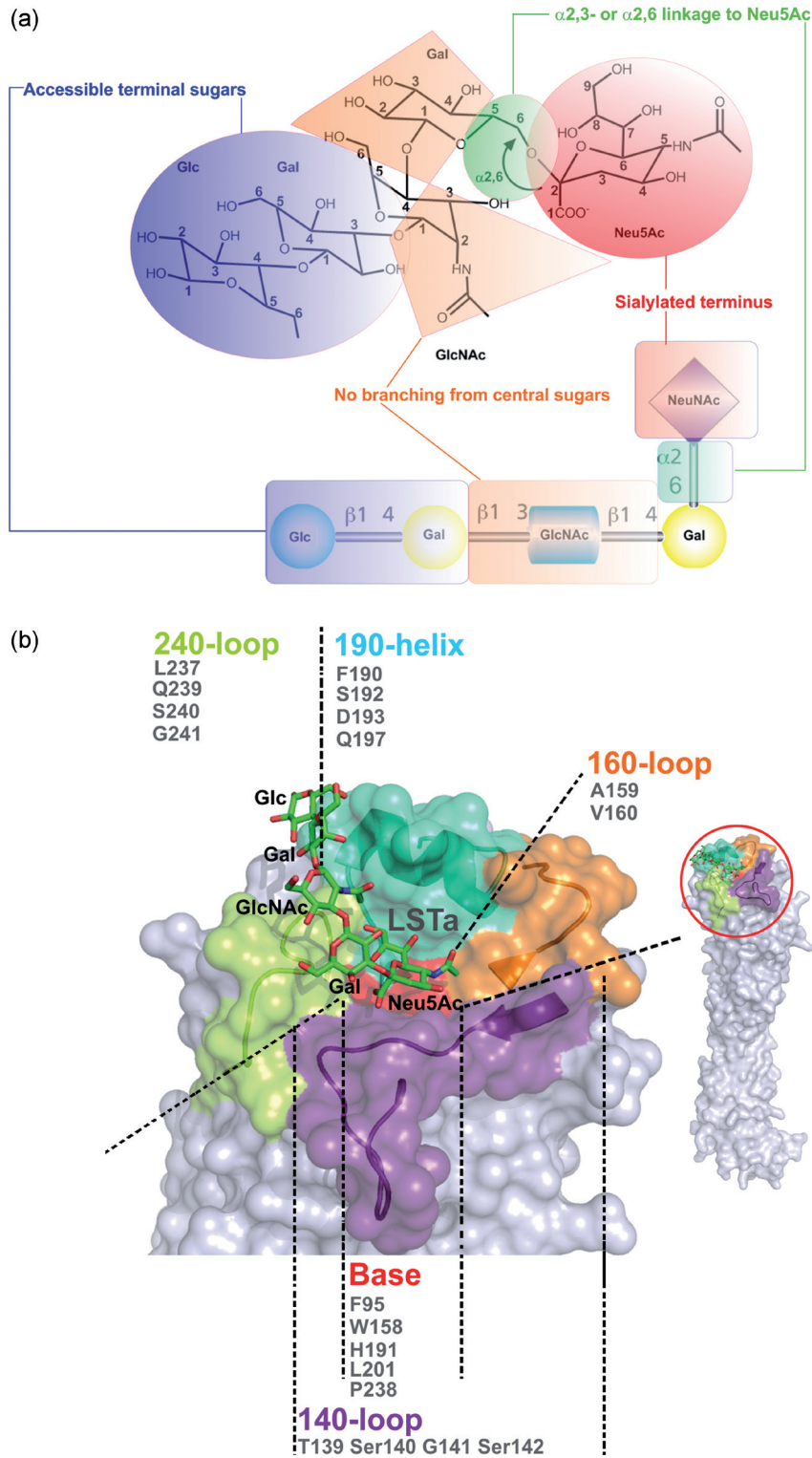


Fig. 4

(a) Structure-activity relationships for influenza B HA receptor recognition. The chemical structure of the human receptor analog LSTc is shown. Below. Schematic diagram showing the monosaccharide composition and arrangement of LSTc. Key to monosaccharides: Neu5Ac = α -N-acetylneuramic acid; Gal = β -D-galactose; GlcNAc = β -D-N-acetyl glucosamine; β -D-Glc = Glucose. (b) General architecture of the influenza B HA receptor-binding pocket. The bound avian receptor analog LSTa is shown in stick representation.

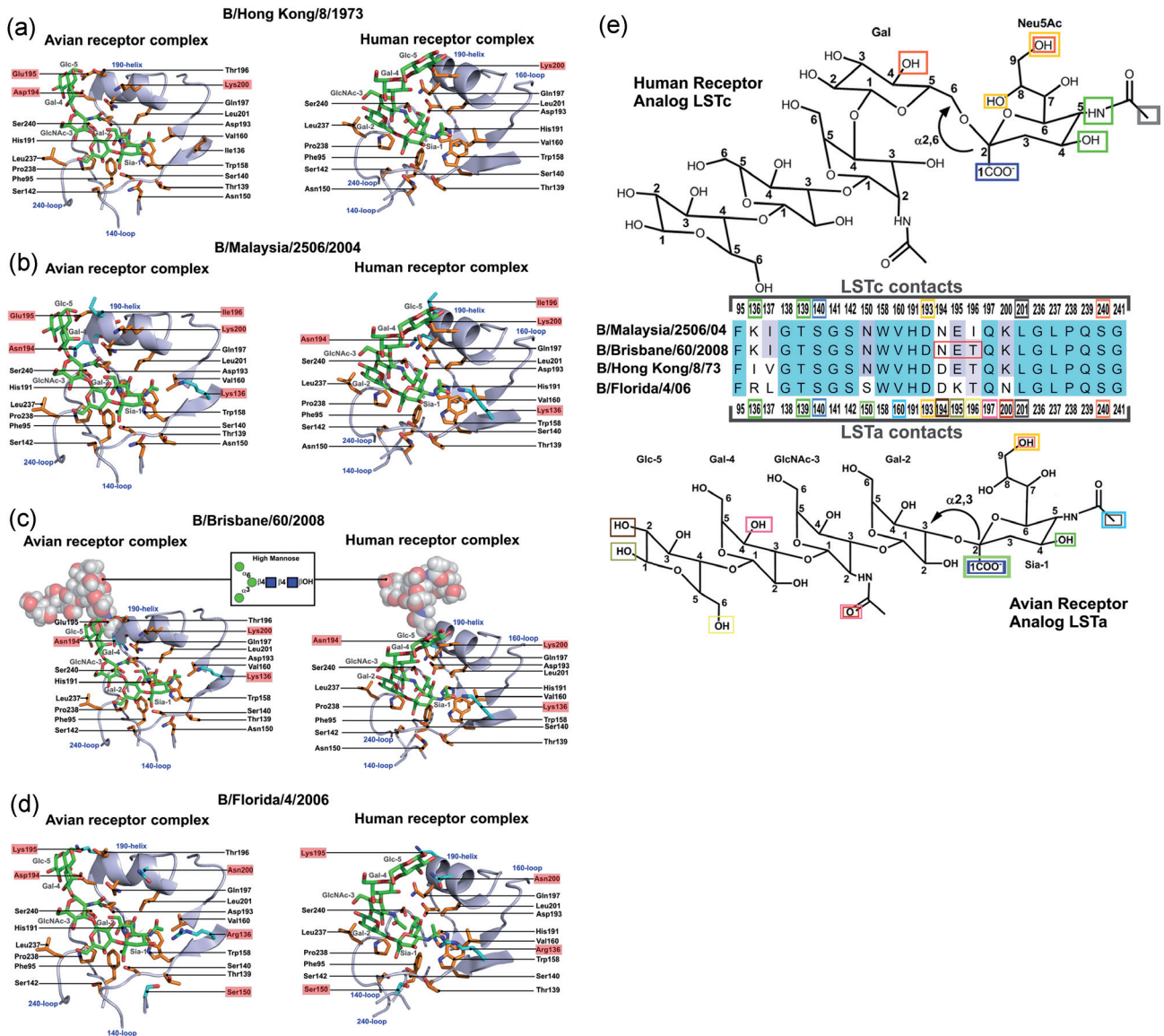


Fig. 5

(a-d) Homology-based structural models of the influenza B HA receptor-binding pockets of B/Malaysia/2506/04/2004, B/Florida/4/2006 and B/Brisbane/60/2008. Models were constructed using the crystallographic avian and human receptor analog complexes of B/Hong Kong/8/1973 HA as the modeling templates. Amino acid side-chains involved in key contacts with the avian (LSTa) and human (LSTc) receptor analogs are shown in stick representation. The labels of amino acid positions that differ from the binding pocket of the experimental are highlighted in red. The modeled high mannose glyco-conjugate on Asn 194 of B/Brisbane/60/2008 is shown in space filling sphere representation (carbon grey). The inset shows the sugar composition of the glycan, with green circles representing mannose units and blue squares representing N-acetylglucosamine units. (e) A color-coded schematic diagram depicting the sequence alignment of the influenza B HA receptor-binding pocket amino acids and the corresponding contact points on the human (LSTc) and avian (LSTa) receptor analog structures. The glycosylation site in the sequence of B/Brisbane/60/2008 is boxed in red.

required to faithfully measure the receptor selectivity of the influenza B HA. Preferably, the assay system should use free pentasaccharide receptor analogs in solution as per the ELISA and our gel-capture competition as-

say platforms. v) TheNeuNAc-1-Gal-2 unit needs to be terminally located if the analog is to serve as a binding substrate. Branched or internalized NeuNAc structures are not tolerated.

Table 2. Individual PLP fitness scores for influenza B HA RBS residues and their interaction with LSTa following *in silico* docking with Gold

		PLP fitness score			
		Malaysia	Florida	Hongkong	Brisbane
	Total Score	38.07	37.67	25.51	18.78
Highly conserved residues	Phe95	1.66	1.23	0.08	1.07
	Thr139	4.08	5.18	3.74	0.83
	Ser140	9.38	10.55	8.83	1.77
	Gly141	4.35	5.37	3.66	3.22
	Trp158	5.4	3.96	4.17	0
	His191	0.97	1.16	0.71	0
	Gln197	0.38	0.16	0.8	1.37
	Leu201	2.58	2.43	1.56	3.36
	Leu237	2.53	3.59	0.03	2.27
	Pro238	2.93	2.88	1.19	4.01
Less conserved residues	Asn150/Ser150/Asn150/Asn150	0.53	0.11	0.07	0.84
	Lys200/Asn200/Lys200/ Lys200	1.19	0	0	0
	Lys136/Arg136/Ile136/Lys136	0.08	1.5	0.56	0.06

Structure-recognition characteristics of influenza B HA regional variants examined through in silico docking and modeling

The high percentage sequence identity (PID) (May, 2004) between the three influenza B HA variants and B/Hong Kong/8/1973 (PID = 93.4 %; Length of alignment = 516; Sequence length = 516), allows the crystallographic structures of the B/Hong Kong/8/1973 HA in complex with LSTa and LSTc to serve as excellent templates for the construction of homology models. In the B/Hong Kong/8/73-LSTc crystal complex the electron density for the distal asialyl Gal-4-Glc-5 sugars of LSTc was very poor (Wang *et al.*, 2007). The unique U shaped configuration and flexibility of LSTc and the solvent-exposed nature of Gal-4-Glc-5 may have been responsible for the poor electron density observed in the B/Hong Kong/8/73-LSTc crystal complex. Accordingly, we have had to model the distal asialyl Gal-4-Glc-5 sugars of LSTc for the docking simulations. In any case, no direct contact was established or observed in our models with the Gal-4-Glc-5 sugars remaining surface exposed. (cf. Fig. 5a–d). Table 3 documents the internal scoring functions for the LSTa docking into each HA, which coincide with the LSTa binding affinities measured for each HA B/Malaysia/2506/2004>B/Florida/4/2006>B/Brisbane/60/2008).

Topographically, the receptor-binding pocket is an indentation on the top of the membrane-distal tip of the influenza B HA molecule (Fig. 4b). The pocket is formed by four secondary structural elements, the 140-, 160-, 240-loops and the 190-helix, that also form a large continuous antigenic site (Wang *et al.*, 2007, 2008). The following section discusses the receptor recognition characteristics of amino acid positions that are highly conserved within the RBS of influenza B HAs

and the three variants under study. Five highly conserved residues, Phe95, Trp158, His191, Leu201 and Pro238 form the base of the pocket (Fig. 4b) (Wang *et al.*, 2007). Additional conserved residues that form the receptor-binding surface include Thr139, Ser140, Gly141, Ser142, Trp158, Ala159, Val160, Phe190, Ser192, Asp193, Gln197, Leu237, Gln239 and Ser240 (Fig. 4b and Table 3). In line with the B/Hong Kong/8/1973 crystallographic complexes, the docking models show that the bound human receptor analog LSTc adopts a U-shaped configuration, whereas the avian analog LSTa has an extended conformation and exits the binding pocket on the C-terminal side of the 190-helix (Fig. 5a–d). Most of the residues that bind the Neu5A-1 moiety of the LST analogs in the crystal structure template are highly conserved across most influenza B virus isolates, including the variants under study (Fig. 5e and Table 3). In the LSTc docking models, the 9-hydroxyl group on the glycerol moiety of Neu5A-1 hydrogen bonds with the side chains of Asp193 and Ser240 (Fig. 5a–d). The main chain amide and carbonyl of Thr139 hydrogen bond to the acetamide moiety and the 4-hydroxyl of Neu5A-1. The carboxyl of Neu5A-1 hydrogen bonds the side chain hydroxyl of Ser140. A Van der Waals contact is made between the hydrophobic side chain of Leu201 and the methyl group on the acetamide moiety of Neu5A-1. Most of the interactions with Neu5A-1-Gal-2 of LSTc are also made with the Neu5A-1-Gal-2 of LSTa, which is consistent with the SAR model, which suggests that the configuration of the Neu5A-1-Gal-2 glycosidic linkage makes only a modest contribution towards binding selectivity. The common contacts with the Neu5A-1-Gal-2 segment of both LST analogs may account for the inability of the HAs to discriminate between the α 2,3 and α 2,6 trisaccharide analogs as these analogs only offer one additional sugar unit for recognition. The only ad-

Table 3. Analysis of the frequency of amino acid substitutions within the receptor-binding pocket of the influenza B HA population

Consensus sequence												
AA position	95	136	137	138	139	140	141	142	150	158	159	160
REGION												
AFRICA	F	R	L	G	T	S	G	S	I	W	A	V
EUROPE	F	R	L	G	T	S	G	S	S	W	A	V
ASIA	F	K	I	G	T	S	G	S	N	W	A	V
OCEANIA	F	R	L	G	T	S	G	S	S	W	A	V
SOUTH AMERICA	F	K	I	G	T	S	G	S	N	W	A	V
NORTH AMERICA	F	R	L	G	T	S	G	S	S	W	A	V
Substitution frequency (% total sequences)												
AA position	95	136	137	138	139	140	141	142	150	158	159	160
F	99.9%	51.3%	51.9%	100%	99.8%	100%	98.3%	100%	49.9%	99.9%	99.3%	99.8%
Y	0.03%	47.1%	46.3%		0.09%		1.08%		41.1%	0.03%	0.59%	0.16%
		I	V		I		E		I		T	R
		1.40%	1.80%		0.06%		0.06%		7.46%		0.06%	0.03%
		T					A		K		S	
		0.17%					0.03%		0.24%			
		N							T			
		0.03%							0.33%			
									D			
									0.21%			
									R			
									0.06%			
									F			
									0.06%			
									E			
									0.03%			
									V			
									0.03%			
Consensus sequence												
AA position	191	192	193	194	195	196	197	200	201			
REGION												
AFRICA	H	S	D	N	K	T	Q	N	L			
EUROPE	H	S	D	N	K	T	Q	N	L			
ASIA	H	S	D	N	E	T	Q	K	L			
OCEANIA	H	S	D	N	K	T	Q	N	L			
SOUTH AMERICA	H	S	D	N	E	T	Q	K	L			
NORTH AMERICA	H	S	D	N	K	T	Q	N	L			
Substitution frequency (% total sequences)												
AA position	191	192	193	194	195	196	197	200	201			
H	99.9%	99.8%	99.9%	92.8%	52.6%	89.6%	99.7%	51.8%	99.7%			
Q	0.03%	0.13%	0.03%	3.37%	47.1%	4.56%	0.19%	46.8%	0.13%			
S	0.03%	0.03%		2.00%	0.13%	3.18%	0.09%	0.44%	0.09%			
		T		K	R	N	H	R	H			
		0.03%		0.73%	0.09%	1.68%	0.03%	0.31%	0.06%			
				Y	A	P	R	I	V			
				0.28%	0.06%	0.71%	0.03%	0.09%	0.03%			
				I	G	S		S	R			
				0.28%	0.03%	0.1%		0.06%	0.03%			
				T		V			S			
				0.25%		0.06%			0.03%			
				H		Y						
				0.13%		0.03%						

Table 3. (continued)

AA position	Consensus sequence					
	236	237	238	239	240	241
REGION						
AFRICA	G	L	P	Q	S	G
EUROPE	G	L	P	Q	S	G
ASIA	G	L	P	Q	S	G
OCEANIA	G	L	P	Q	S	G
SOUTH AMERICA	G	L	P	Q	S	G
NORTH AMERICA	G	L	P	Q	S	G
Substitution frequency (% total sequences)						
AA position	236	237	238	239	240	241
	G	L	P	Q	S	G
	100%	99.9 %	99.6 %	99.9%	100 %	100 %
		I	K	P		
		0.03%	0.25%	0.03 %		
		R 0.03%	S			
			0.06%			
		Q	Q			
		0.03 %	0.06%			

ditional contacts made with the Neu5A-1 of LSTa that are not seen with the Neu5A-1 of LSTc, are between the side chain of Asn150 (Ser150 in B/Florida/4/2006) and the Neu5A-1 carboxyl and a Van der Waals contact between the side chain of Val160 with the methyl group of the Neu5A-1 acetamide moiety (Fig. 5).

The docking models clearly show that binding of the LST receptor analogs involves an extensive series of contacts over the entire length of the oligosaccharide, which may account for the inability of the HA to bind Neu5A *per se*. Potentially, the Neu5A-1-Gal-2 segment acts a nucleation site, following which the rest of the oligosaccharide binds in a sequential fashion. Such a mechanism would also account for the necessity of the Neu5A-1-Gal-2 segment to be terminally located and the absence of binding seen when using analogs with branched or internal Neu5A moieties (LSTb, SLFPI and MSLNH).

Having established the common architectural features of the influenza B HA receptor-binding pocket, we now discuss how regional HA-lineage-specific substitutions in the variants under study at key positions 136–137, 150, 194–196, and 200 can influence receptor selectivity and avidity. In regards to positions 136–137, position 137 is distal from the bound receptor, whereas the side chain of position 136 makes contacts with Neu5A-1 in both LSTa and LSTc (Fig. 5). The HA of B/Malaysia/2506/2004 and B/Brisbane/60/2008 displays the Lys136-Ile137 motif, which is typical of Asian and South American strains representative of the B/Victoria/2/1987 lineage, whereas B/Florida/4/2006 displays the Arg136-Leu137 motif, which is typical of the African, European, Oceania and North American regional strains that are representative of the B/Yamagata/16/88 lineage (Table 3).

In B/Malaysia/2506/2004 and B/Brisbane/60/2008 the side chain of Lys136 hydrogen bonds with the 4-hydroxyl of Neu5A-1 (Fig. 5b, c), whereas the Arg136 guanidinyll side chain in B/Florida/4/2006 hydrogen bonds with both the 4-hydroxyl and acetamide moiety of Neu5A-1 (Fig. 5d). In addition to these two common lineage-specific 136–137 motifs, Thr136-Val137, Ile136-Val137, and Asn136-Leu137 are less commonly observed in the influenza B HA population (Table 3). In view of the models, it is apparent that the side chains of Thr, Ile or Asn would be too short to make contact with the Neu5A-1. This is exemplified in B/Hong Kong/8/73 crystallographic LST complexes, where the side chain of Ile136 is too short to make contacts with the Neu5A-1 acetamide moiety (Fig. 4a). The inability to contact the Neu5A-1 acetamide moiety would render the right-hand horizontal border of the pocket much wider when compared to the Arg or Lys side chains and dramatically reduce binding efficiency.

The B/Hong Kong/8/73-LSTa crystal structure reveals that the extended conformation of the avian receptor analog LSTa arises from rotation of GlcNAc-3 around the Gal-2-GlcNAc-3 bond by approximately 60°, which bends the Gal-4 and Glc-5 units towards the 190-helix and allows for interactions with the side chains of residues 194–196 (Fig. 5a) (Wang *et al.*, 2007). Taken together with the SAR data, the models suggest that the interaction between the 194–196 side chains and the distal asialyl Gal-4-Glc-5 sugars constrains receptor preference and modulates LSTa avidity between HA variants. Contacts between the asialyl sugar units of LSTa and the 190-helix side chains include hydrogen bonds between the 4-hydroxyl group of Gal-4 and the side-chains of Asp193 and Gln197, which are both highly conserved positions. The

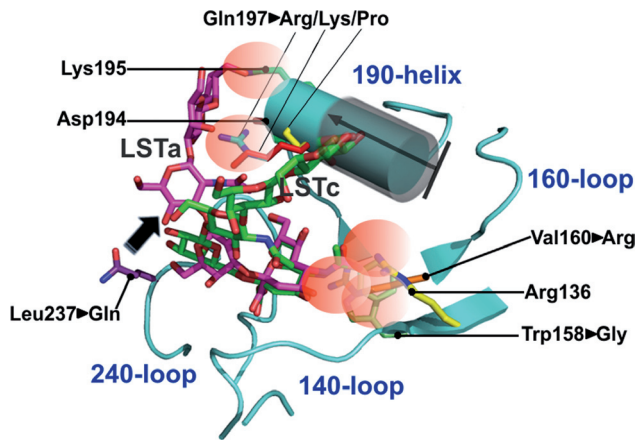


Fig. 6

Naturally occurring mutations in the influenza B HA pocket that would limit the binding of the human receptor analog LSTc modeled onto the receptor-binding pocket of the B/Hong Kong/8/1973-LST crystallographic complex. Amino acid side chains and LST analogs are shown in stick representation. The receptor-binding pocket secondary structural elements are shown in ribbon representation.

side chains of residues Gln197 and residue 200 (Lys200 in B/Malaysia/2506/2004 and B/Brisbane/60/2008; and Asn200 in B/Florida/4/2006) are within hydrogen-bonding distance of the GlcNAc-3 acetamide moiety (Fig. 5b-d). The Glc-5 sugar makes extensive contacts with the side chain of residues 194–196 (Asn194-Glu195-Ile196 in B/Malaysia/2506/2004; Asn194-Glu195-Thr196 in B/Brisbane/60/2008; Asp194-Lys195-Thr196 in B/Florida/4/2006; Asp194-Glu195-Thr196 in B/Hong Kong/8/1973). The receptor pocket models also indicate that recognition of human type receptors is largely dependent on interactions with the first two-to-three sugar units, this contrasts the recognition of avian type receptors, which is strongly dependent on contacts with the distal asialyl sugars. This mechanism would account for the weaker discriminating power of the trisaccharide analogs compared to their pentasaccharide counterparts.

The Victoria influenza B strains are predominantly glycosylated at position 194–196 in the RBS (as per B/Brisbane/60/2008), whereas the Yamagata strains are predominately non-glycosylated (as per B/Florida/4/2006). Although B/Malaysia/2506/2004 belongs to the Victoria lineage, it lacks the N-glycosylation at the position 194–196. Based on a sequence comparison, the only difference between the binding pocket sequences of Malaysia/2506/2004 and B/Brisbane/60/2008 occurs at position 194–196, wherein Thr196 (B/Brisbane/60/2008) is substituted for Ile196 (B/Malaysia/2506/2004), representing the loss of glycosylation at this site in B/Malaysia/2506/2004 (Fig. 5e). The model of B/Brisbane/60/2008 highlights the negative steric effects of a glyco-conjugate attached to the side chain of Asn194 on the

190-helix (Fig. 4c). This model suggests that the carbohydrate structure sterically hinders the exit path of LSTa by interfering with binding of the distal asialyl Gal-4-Glc-5 sugars and may account for the reduced avidity of B/Brisbane/60/2008 for the avian receptor analogs 3'SL and LSTa, and its inability to effectively bind to analogs that are coupled to a solid-phase support by attachment to the terminal sugars (Table 1). In contrast, in the U-shaped configuration of the human receptor analog LSTc, the distal asialyl Gal-4-Glc-5 sugars are not hindered by the glycol-conjugate. This is reflected in the ability of B/Brisbane/60/2008 to bind LSTc with comparable affinity to B/Malaysia/2506/2004 and B/Florida/4/2006 strains, which lack the Asn194 glyco-conjugate (Fig. 5c).

Of the three test strains, B/Malaysia/2506/2004 displayed the most promiscuous receptor-binding characteristics, showing an almost comparable affinity for both avian and human receptor analogs. The B/Malaysia/2506/2004 model suggests that the Thr196→Ile substitution, which results in loss of the glycol-conjugate at the position 194, widens the C-terminal 190-helix end of the binding pocket, provides greater accommodation for the extended LSTa analog and facilitates recognition of the terminal sugars (Fig. 5b). In contrast, modeling of B/Florida/4/2006-LSTa interaction indicates that naturally occurring substitutions commonly observed in the HA binding pocket of the African, European, Oceania and North American regional strains, exemplified by B/Florida/4/2006, limit contacts with the asialyl Gal-4-Glc-5 sugars and obstruct its ability to attain the extended conformation (Fig. 5d). The narrowing of the horizontal borders of the binding pocket by the Asp194-Lys195 substitutions in the C-terminal 190-helix end, and the Arg136 substitution near the N-terminal end of the 140-loop restrain the ability of the avian receptor to enter the pocket and account for the stricter α ,6 analog selectivity of B/Florida/4/2006 HA (Fig. 5d).

In order to help understand how certain naturally occurring substitutions in the influenza B HA population impact receptor recognition, we mapped these substitutions onto the B/Hong Kong/8/1973-LST crystallographic complex (Fig. 6). The binding pocket model depicts how the long guanidinyll side chain of Arg136 and the side chains of Asp194-Lys195 of the HA pocket act synergistically to make the pocket less accommodating for the extended conformation of LSTa and to block its exit path (Fig. 6). With respect to the 190-helix, the Asn200 side chain of B/Florida/4/2006 is too short to contact with the asialyl sugars of LSTa, whereas the longer Lys200 side chain of B/Malaysia/2506/2004 and B/Brisbane/60/2008 is able to make favorable stabilizing contacts with the acetamide group of GlcNAc-3 (Fig. 5b-d). Although Gln197 is highly conserved across the influenza B HA population (Table 3), we detected a number of strains in the database that exhibit either Lys (B/Philippines/clinical isolate SA64/2002; GenBank Acc. No. AAY21738), Arg

(B/Nanchang/3451/93; GenBank accession no. AAD02807) or Pro (B/Jilin/20/20; GenBank Acc. No. ABO37785) substitutions at this position. Modeling indicates that the long side chains of Lys197 or Arg197 block the left side of the pocket and hinder the asialyl contacts, upon which LSTa is highly dependent upon for recognition, whereas Pro197 truncates the 190-helix to eliminate key residues involved in recognition of the asialyl terminus of LSTa (Fig. 6). These substitutions, therefore, significantly narrow the horizontal borders of the receptor-binding cleft. In summary, the naturally occurring substitutions in the 190-helix (Asn194 glycosylation, Asp194-Lys195, Glu197→Lys/Arg/Pro) of the influenza B HA population allow the viral HA to restrain binding of avian receptors, while concomitantly making the pocket more adept for binding of human receptors.

Whilst our modeling covers the structure-recognition characteristics of all naturally occurring amino acid substitutions in the receptor-binding pocket of the influenza B HA population; a Leu237→Gln mutation within the HA receptor-binding pocket, which results in zanamivir resistance in influenza A and B viruses, has been observed under laboratory conditions (McKimm-Breschkin *et al.*, 1996, 1998). The HA of these viruses exhibit a lower affinity of the viral HA for cell surface sialyl-glycan receptors and an attenuated ability to absorb and penetrate cells, thereby reducing the dependency on neuraminidase for viral replication (McKimm-Breschkin *et al.*, 1996, 1998). The HA Leu237 residue is highly conserved in influenza B viruses, with only an isolated report of a Leu237→Ile conservative substitution in a clinical isolate having been observed (B/Fukuoka/80/1981; GenBank Acc. No. AAA43691). The importance of Leu237 for receptor binding is highlighted by its high PLP fitness score (Table 2). Modeling indicates that the longer side chain of Gln237 would push the Gal-2 unit forward, such that both the avian and human receptor analogs would sit much higher up in the binding pocket, and thereby reduce the binding affinity (Fig. 6). This contrasts to the deeper Gal-2 position in the B/Hong Kong/8/1973 crystallographic complexes, where hydrogen bonding between Gal-2 and the main chain carbonyl of Leu237 pulls the entire LST molecule to sit in a lower position within the binding pocket (Fig. 5a).

Sequence analysis of the influenza B HA receptor-binding pocket

Based on the B/Hong Kong/8/1973 HA crystallographic structure we can discern that the receptor-binding pocket of the influenza B HA is formed by six discontinuous sequence elements that include positions 95, 136–142, 150, 158–160, 191–201, and 236–241 (Fig. 4b and Table 3). In order to define the frequency and nature of amino acid substitutions within the receptor-binding pocket we performed a sequence analysis

of all human influenza B HAs in the NCBI influenza database as of Nov 2011 (Table 3). All regional strains displayed Phe at position 95, the sequence analysis of all influenza B HAs in the database revealed only one conservative substitution of Tyr95 in B/Indiana/5/2006 (GenBank Acc. No. Q0A1E5). The analysis of the next element at positions 136–142 reveals that Asian and South American strains representative of the B/Victoria/2/1987 lineage displayed the Lys136-Ile137 motif, whereas the remaining regional strains representative of the B/Yamagata/16/88 lineage, displayed the Arg136-Leu137 motif (Table 3). The remaining segment of the 136–142 element Gly138-Thr139-Ser140-Gly141-Ser142 is highly conserved across all strains, with the only notable substitution being Gly141→Arg commonly seen in egg-adapted strains (Lugovtsev *et al.*, 2009). Position 150 shows some variability, in the Asian and South American strains Asn is the most common substitution, representing ~50 % of the total population. In contrast, in the European, North American and Oceania strains, the position 150 is most commonly occupied by Ser, which represents ~41% of the total population. The African strains most commonly exhibited an Ile at this position representing ~7.5% of the total population. The 158–160 sequence element is highly conserved, with Trp158-Ala159-Val160 constituting the majority of the sequence population. The only notable substitutions include Trp158→Gly in B/Kentucky/01/2007 (GenBank Acc. No. ACA33485) and Val160→Arg in B/Uruguay/NG/2002 (GenBank Acc. No. Q08GG5), which, based on the position and the nature of the side chain of the substitutions, are expected to impact on the recognition of the terminal Neu5Ac unit. The 191–201 element forms the 190 helix 'roof' of the binding pocket and harbors an important glycosylation site, Asn194-X-Thr196. The 191–193 part of the element is highly conserved with His191-Ser192-Asp193 representing ~99.9 % of the total population. The 194–196 glycosylation site, representing the C-terminal side of the 190-helix, shows a considerable degree of variability across the population. Position 194 is most commonly occupied by Asn (~93 % of the total population), with Asp, Ser, Lys and Tyr, Ile making up the remaining minor fractions of the population. Position 195 is easily distinguishable between the Asian and South American strains, which exhibit a Glu (~47.1 % of the total population), whereas the African, European, Oceania and North American regional strains display a Lys (~52.6 % of the total population). Position 196 is occupied by Thr in most of the population, with Ile and Ala, representative of egg-adaptation mutations, making up the majority of the remaining fraction. Position 197 is highly conserved with Gln representing ~99.7 % of the total population. The Pro substitutions observed at both positions 196 and 197 as a minor fraction of each population are very interesting, as in protein structures Pro commonly acts as a helix terminator, and therefore would act to truncate the 190 helix (cf. Fig. 6). Position 200 is largely occupied by Lys in the Asian and South

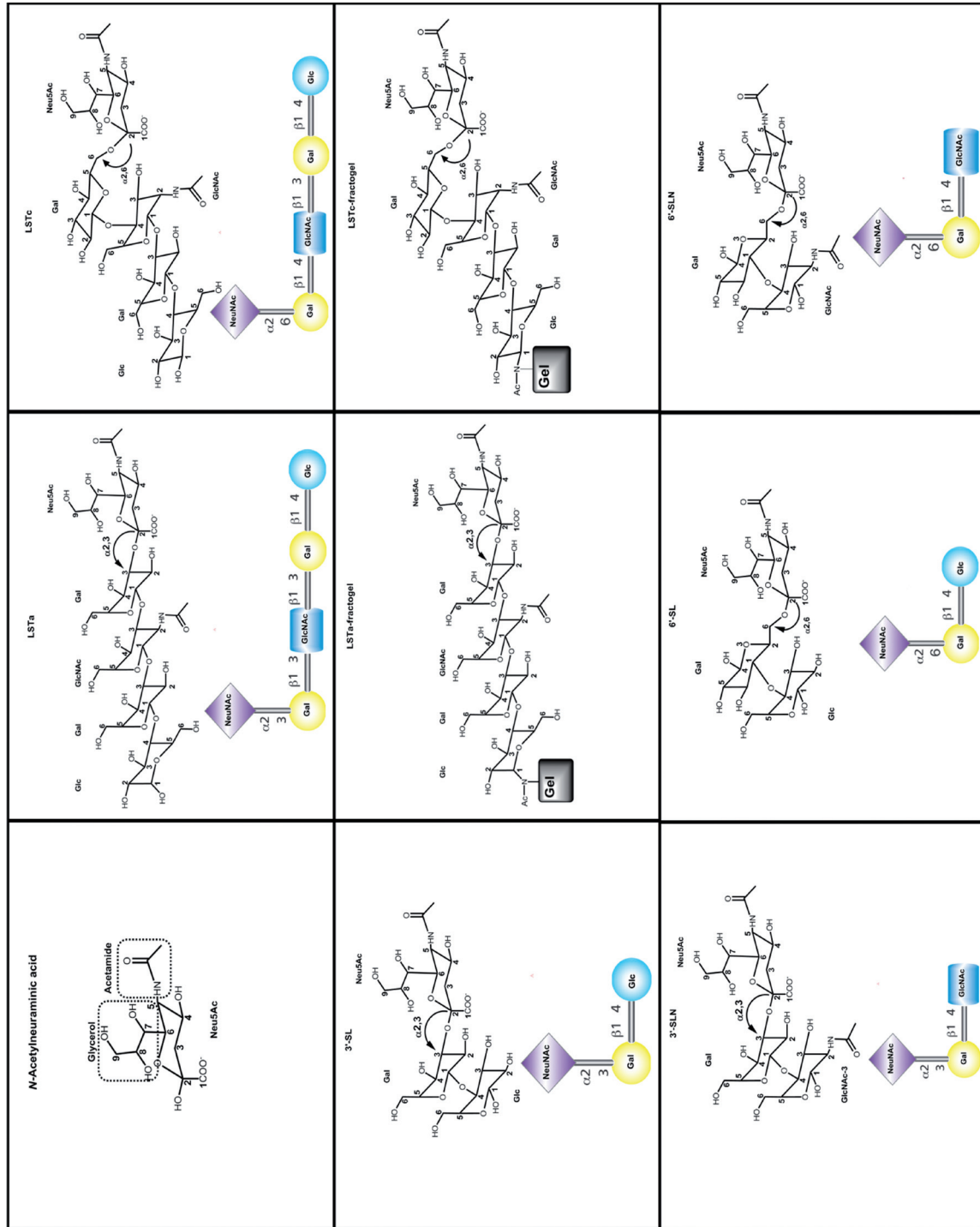


Fig. 7
Chemical structures of the sialyl-oligosaccharides used in this study

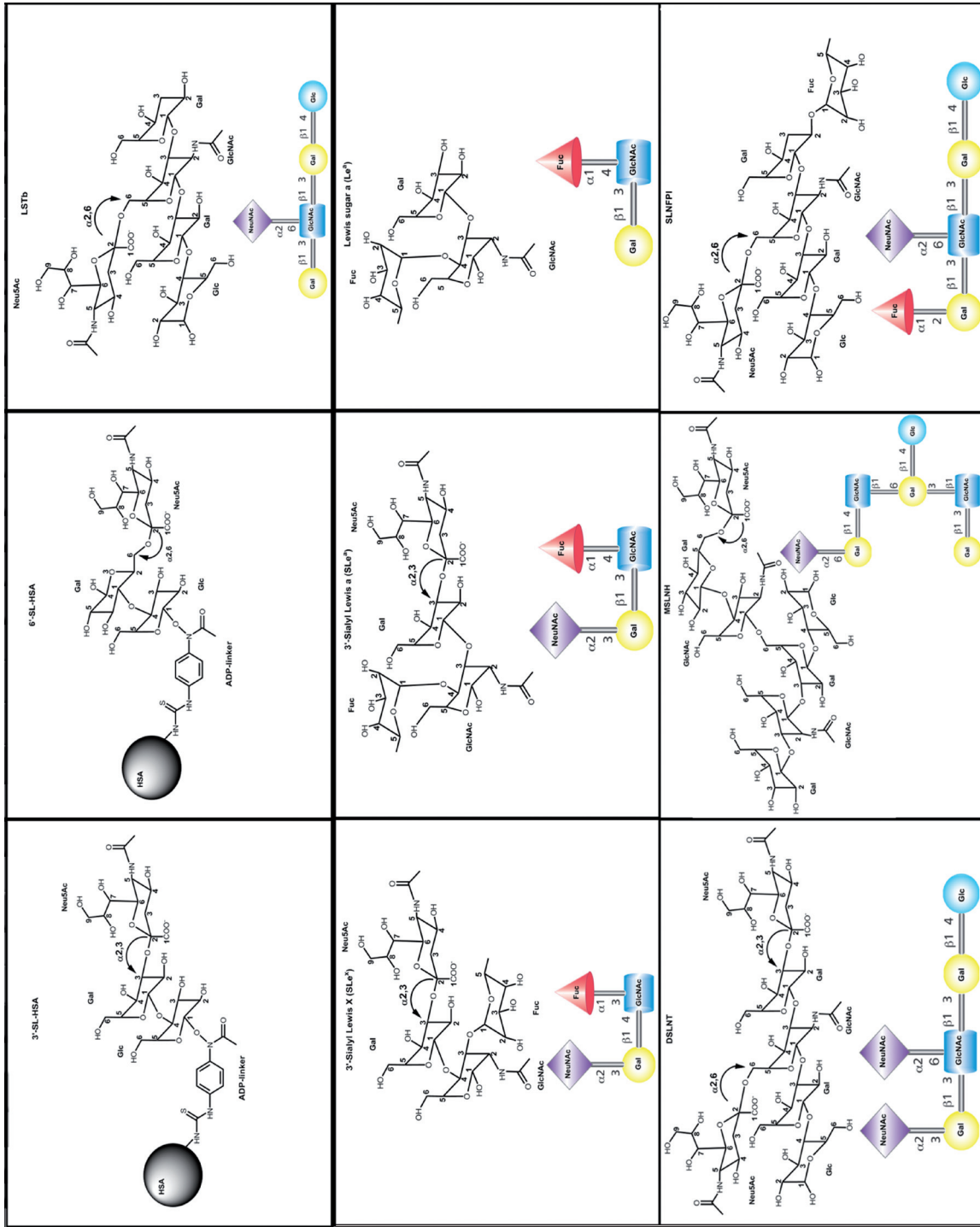


Fig. 7 (continued)

Insets. schematic diagrams showing the monosaccharide composition and arrangement of each compound. Key to monosaccharides: Neu5Ac=α-N-acetylneuramic acid; Gal = β-D-galactose; GlcNAc = β-D-N-acetylglucosamine; β-D-Glc = glucose; Fuc = α-L-fructose.

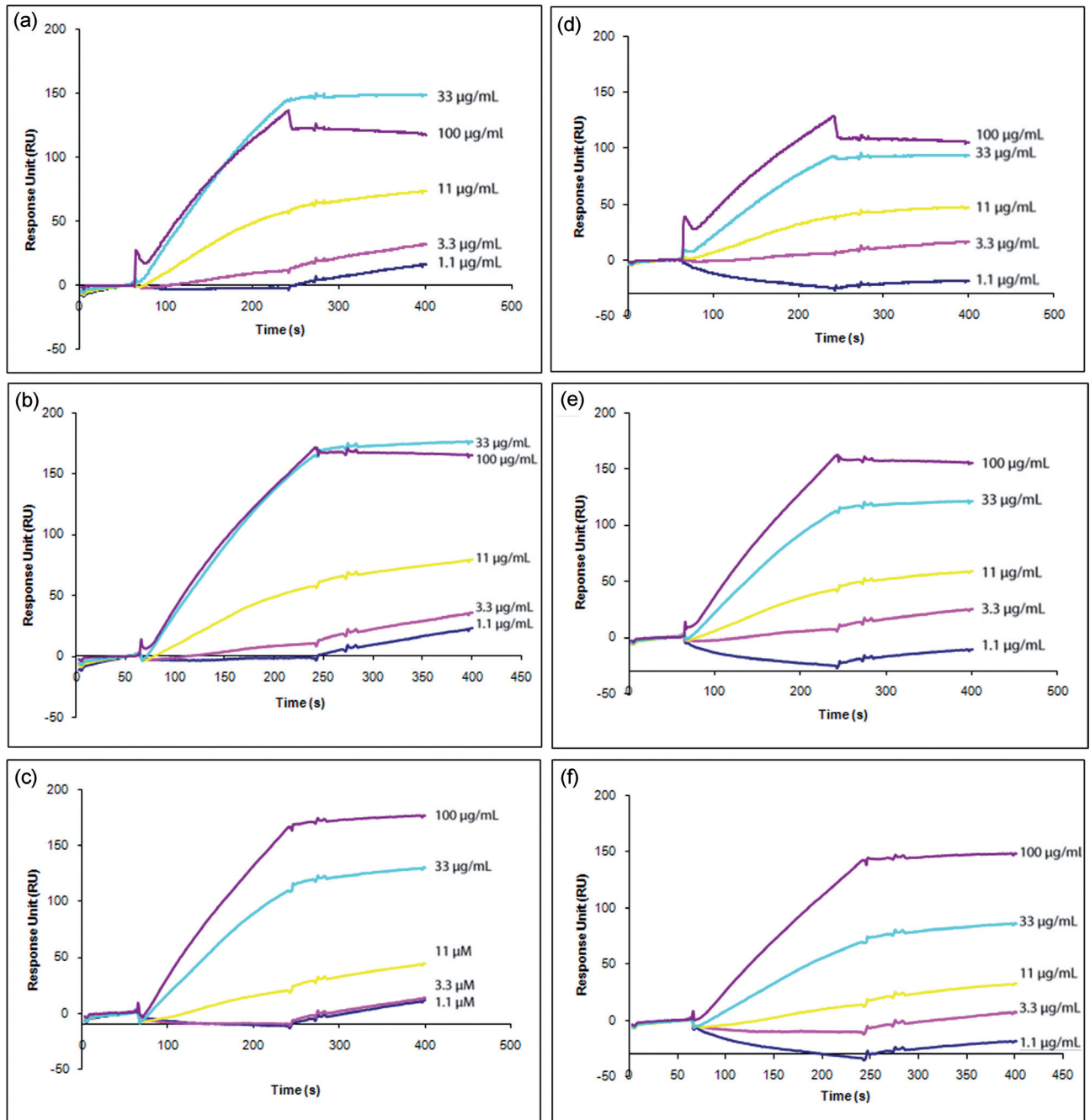


Fig. 8

SPR sensorgrams of HSA conjugated 3'-SL and 6'-SL analogs binding to immobilized influenza B viruses

(a, b, c) show 3'-SL-HSA binding to B/Malaysia/2506/04/04, B/Florida/4/06, and B/Brisbane/60/2008, respectively; (d, e, f) show 6'-SL-HSA binding to B/Malaysia/2506/04/04, B/Florida/4/06, and B/Brisbane/60/2008, respectively.

American strains and Asn in the African, European, Oceania and North American regional strains, with Thr and Arg corresponding to a minor percentage of the sequence population. Position 201 is highly conserved with Leu constituting ~99.7%

of the total population. The 236–241 sequence element is the most highly conserved component of the binding pocket with Gly236-Leu237-Pro238-Gln239-Ser240-Gly241 representing ~99.9→100% of the population.

Acknowledgements. T.V. is a National Health and Medical Research Council of Australia CDA1 Industry Fellow (1003836). This work was supported by the strategic award grant 594875 from the National Health and Medical Research Council of Australia.

References

- Chandrasekaran A, Srinivasan A, Raman R, Viswanathan K, Raguram S, Tumpey TM, Sasisekharan V, Sasisekharan R (2008): Glycan topology determines human adaptation of avian H5N1 virus hemagglutinin. *Nat. Biotechnol.* 26, 107–113. <http://dx.doi.org/10.1038/nbt1375>
- Gambaryan AS, Robertson JS, Matrosovich MN (1999): Effects of egg-adaptation on the receptor-binding properties of human influenza A and B viruses. *Virology* 258, 232–239. <http://dx.doi.org/10.1006/viro.1999.9732>
- Gambaryan AS, Tuzikov AB, Piskarev VE, Yamnikova SS, Lvov DK, Robertson JS, Bovin NV, Matrosovich MN (1997): Specification of receptor-binding phenotypes of influenza virus isolates from different hosts using synthetic sialylglycopolymers: non-egg-adapted human H1 and H3 influenza A and influenza B viruses share a common high binding affinity for 6'-sialyl(N-acetylactosamine). *Virology* 232, 345–350. <http://dx.doi.org/10.1006/viro.1997.8572>
- Gamblin SJ, Haire LF, Russell RJ, Stevens DJ, Xiao B, Ha Y, Vasisht N, Steinhauer DA, Daniels RS, Elliot A, Wiley DC, Skehel JJ (2004): The structure and receptor binding properties of the 1918 influenza hemagglutinin. *Science* 303, 1838–1842. <http://dx.doi.org/10.1126/science.1093155>
- Gatherer D (2010): Passage in egg culture is a major cause of apparent positive selection in influenza B hemagglutinin. *J. Med. Virol.* 82, 123–127. <http://dx.doi.org/10.1002/jmv.21648>
- Hoofst RW, Vriend G, Sander C, Abola EE (1996): Errors in protein structures. *Nature* 381, 272. <http://dx.doi.org/10.1038/381272a0>
- Kanegae Y, Sugita S, Endo A, Ishida M, Senya S, Osako K, Nerome K, Oya A (1990): Evolutionary pattern of the hemagglutinin gene of influenza B viruses isolated in Japan: cocirculating lineages in the same epidemic season. *J. Virol.* 64, 2860–2865.
- Lugovtsev VY, Smith DF, Weir JP (2009): Changes of the receptor-binding properties of influenza B virus B/Victoria/504/2000 during adaptation in chicken eggs. *Virology* 394, 218–226. <http://dx.doi.org/10.1016/j.virol.2009.08.014>
- Matrosovich MN, Gambaryan AS, Tuzikov AB, Byramova NE, Mochalova LV, Golbraikh AA, Shenderovich MD, Finne J, Bovin NV (1993): Probing of the receptor-binding sites of the H1 and H3 influenza A and influenza B virus hemagglutinins by synthetic and natural sialosides. *Virology* 196, 111–121. <http://dx.doi.org/10.1006/viro.1993.1459>
- May AC (2004): Percent sequence identity; the need to be explicit. *Structure* 12, 737–738. <http://dx.doi.org/10.1016/j.str.2004.04.001>
- McKimm-Breschkin JL, McDonald M, Blick TJ, Colman PM (1996): Mutation in the influenza virus neuraminidase gene resulting in decreased sensitivity to the neuraminidase inhibitor 4-guanidino-Neu5Ac2en leads to instability of the enzyme. *Virology* 225, 240–242. <http://dx.doi.org/10.1006/viro.1996.0595>
- McKimm-Breschkin JL, Sahasrabudhe A, Blick TJ, McDonald M, Colman PM, Hart GJ, Bethell RC, Varghese JN (1998): Mutations in a conserved residue in the influenza virus neuraminidase active site decreases sensitivity to Neu5Ac2en-derived inhibitors. *J. Virol.* 72, 2456–2462.
- Nerome R, Hiromoto Y, Sugita S, Tanabe N, Ishida M, Matsumoto M, Lindstrom SE, Takahashi T, Nerome K (1998): Evolutionary characteristics of influenza B virus since its first isolation in 1940: dynamic circulation of deletion and insertion mechanism. *Arch. Virol.* 143, 1569–1583. <http://dx.doi.org/10.1007/s007050050399>
- Robertson JS, Nicolson C, Major D, Robertson EW, Wood JM (1993): The role of amniotic passage in the egg-adaptation of human influenza virus is revealed by haemagglutinin sequence analyses. *J. Gen. Virol.* 74, 2047–2051. <http://dx.doi.org/10.1099/0022-1317-74-10-2047>
- Rota PA, Hemphill ML, Whistler T, Regnery HL, Kendal AP (1992): Antigenic and genetic characterization of the haemagglutinins of recent cocirculating strains of influenza B virus. *J. Gen. Virol.* 73, 2737–2742. <http://dx.doi.org/10.1099/0022-1317-73-10-2737>
- Saito T, Nakaya Y, Suzuki T, Ito R, Saito H, Takao S, Sahara K, Odagiri T, Murata T, Usui T, Suzuki Y, Tashiro M (2004): Antigenic alteration of influenza B virus associated with loss of a glycosylation site due to host-cell adaptation. *J. Med. Virol.* 74, 336–343. <http://dx.doi.org/10.1002/jmv.20178>
- Skehel JJ, Wiley DC (2000): Receptor binding and membrane fusion in virus entry: the influenza hemagglutinin. *Annu. Rev. Biochem.* 69, 531–569. <http://dx.doi.org/10.1146/annurev.biochem.69.1.531>
- Srinivasan A, Viswanathan K, Raman R, Chandrasekaran A, Raguram S, Tumpey TM, Sasisekharan V, Sasisekharan R (2008): Quantitative biochemical rationale for differences in transmissibility of 1918 pandemic influenza A viruses. *Proc. Natl. Acad. Sci. USA* 105, 2800–2805. <http://dx.doi.org/10.1073/pnas.0711963105>
- Stevens J, Blixt O, Glaser L, Taubenberger JK, Palese P, Paulson JC, Wilson IA (2006a): Glycan microarray analysis of the hemagglutinins from modern and pandemic influenza viruses reveals different receptor specificities. *J. Mol. Biol.* 355, 1143–1155. <http://dx.doi.org/10.1016/j.jmb.2005.11.002>
- Stevens J, Blixt O, Tumpey TM, Taubenberger JK, Paulson JC, Wilson IA (2006b): Structure and receptor specificity of the hemagglutinin from an H5N1 influenza virus. *Science* 312, 404–410. <http://dx.doi.org/10.1126/science.1124513>
- Stevens J, Blixt O, Chen LM, Donis RO, Paulson JC, Wilson IA (2008): Recent avian H5N1 viruses exhibit increased propensity for acquiring human receptor specificity. *J.*

- Mol. Biol. 381, 1382–1394. <http://dx.doi.org/10.1016/j.jmb.2008.04.016>
- Suzuki Y (2005): Sialobiology of influenza: molecular mechanism of host range variation of influenza viruses. *Biol. Pharm. Bull.* 28, 399–408. <http://dx.doi.org/10.1248/bpb.28.399>
- Szretter KJ, Balish AL, Katz JM (2006): Influenza: propagation, quantification, and storage. *Curr. Protoc. Microbiol.* John Wiley & Sons, Ltd Chapter 15, Unit 15G 1.
- Thompson JD, Higgins DG, Gibson TJ (1994): CLUSTAL W: improving the sensitivity of progressive multiple sequence alignment through sequence weighting, position-specific gap penalties and weight matrix choice. *Nucleic Acids Res.* 22, 4673–4680. <http://dx.doi.org/10.1093/nar/22.22.4673>
- Velkov T, Thompson PE, El-Kabbani O, Lindh F, Stambas J, Rockman S (2011): A gel-capture assay for characterizing the sialyl-glycan selectivity of influenza viruses. *Acta Virol.* 55, 131–137. http://dx.doi.org/10.4149/av_2011_02_131
- Wang Q, Cheng F, Lu M, Tian X, Ma J (2008): Crystal structure of unliganded influenza B virus hemagglutinin. *J. Virol.* 82, 3011–3020. <http://dx.doi.org/10.1128/JVI.02477-07>
- Wang Q, Tian X, Chen X, Ma J (2007): Structural basis for receptor specificity of influenza B virus hemagglutinin. *Proc. Natl. Acad. Sci. USA* 104, 16874–16879. <http://dx.doi.org/10.1073/pnas.0708363104>
- Xu R, Ekiert DC, Krause JC, Hai R, Crowe JE Jr, Wilson IA (2010): Structural basis of preexisting immunity to the 2009 H1N1 pandemic influenza virus. *Science* 328, 357–360. <http://dx.doi.org/10.1126/science.1186430>